Time-domain Simulation of Electric Circuit with Nonlinear Hysteretic Inductor

Srđan Divac and Branko Koprivica

***Abstract*—The aim of this paper is to present a method for simulation of electric circuits with nonlinear inductor with hysteresis in time domain. The method is based on solving equation derived from Kirchhoff's law of the considered electric circuit through a series of successive iterations. Electric circuit consisting of AC voltage source connected in series with linear resistor, linear inductor and nonlinear inductor with hysteresis has been considered. Simulations have been performed for four cases of the considered electric circuit – without linear elements, with one and both linear elements, for sinusoidal voltage source amplitudes from 2 V to 10 V with the step of 2 V. Detailed simulation procedure, measurement and simulation results, as well as adequate discussion, have been presented.**

***Index Terms*—Simulation method, electric circuit, nonlinear inductor, magnetic hysteresis, time domain.**

I. Introduction

SOLVING an electric circuit with nonlinear inductor with hysteresis is very challenging due to the appearance of higher harmonics in the electric current, due to distorted waveform of the magnetic field (strength) of considered inductor [1]. Methods used in power engineering are commonly obtained by substituting the inductor with an equivalent *RL* circuit (consisting of a single nonlinear inductor represented by magnetising curve in parallel with linear or nonlinear resistor to represent hysteresis power loss) and solving the circuit [2]. However, this method cannot accurately solve electric circuits in time domain. Better results in time domain can be obtained by varying the resistance and the inductance of the elements in time, as proposed by De Leon [3]. More complex solutions of the electric circuit implement the use of one of the hysteresis models to represent the inductor with hysteresis [4]. Some of the commonly used models are: Preisach [5], Jilles-Atherton [6], Neural Network based models [7] and others. This method gives better results in time domain but the mathematics behind the model itself can be quite complex and its parameters difficult to obtain.

Presented simulation method is based on solving equation derived from Kirchhoff's law for the considered electric circuit through series of successive iterations. Electric circuit consisting of AC voltage source connected in series with linear resistor, linear inductor and nonlinear inductor with hysteresis. Influence of the inductor with hysteresis has been accounted for by calculating circuit current from dynamic magnetic field waveform $H_{dyn}(t)$ of the inductor. Dynamic field $H_{dyn}(t)$ has been obtained by following the simulation method for dynamic hysteresis loops and rate-independent property of the quasistatic hysteresis loops [8, 9]. This has been done by considering three components of $H_{dyn}(t)$ - quasistatic field $H_{qs}(t)$, eddy current field $H_{eddy}(t)$ and excess field $H_{exc}(t)$ [10].

Measurements of the magnetic field waveform $H(t)$ and magnetic flux density waveform $B(t)$ have been made using the measurement method based on data acquisition with PC [1]. Waveforms have been measured at frequency of 1 Hz for amplitudes of sinusoidal $B(t)$ from 0.2 T to 1.6 T with measurement step of 0.2 T. Also, measurement has been made at frequency of 50 Hz for sinusoidal $B(t)$ with the amplitude of 1 T. This measurement has been used for calculation of phenomenological parameters of $H_{exc}(t)$ by fitting the calculated excess power loss to measured excess loss. Fitting has been performed using the criteria of least root mean square deviation (RMSD [11, 12]) between excess power loss.

Simulations have been made for four cases of the considered electric circuit - without linear elements, with one and both elements, for sinusoidal input voltage with amplitudes from 2 V to 10 V with the step of 2 V.

A description of the simulation procedure, presentation of measurement and simulation results, as well as adequate discussion have been given in the paper.

II. Measurement Results

Measurements of magnetic field $H(t)$ and magnetic flux density $B(t)$ waveforms have been performed by using measurement method based on data acquisition and PC [1]. Measurements have been made with toroidal shaped sample made of electrical steel sheet 27PH100 (manufactured by POSCO). Parameters of used toroidal sample can be found in Table I. All measurements have been made with 1000 data points.

TABLE I
Parameters of the Toroidal Sample

N_1	175	r_1 [mm]	45
N_2	60	r_2 [mm]	52.5
l_c [m]	0,306	m [kg]	0.241
S [mm^2]	102,80	w [mm]	15

A set of quasistatic hysteresis loops has been measured at

Srđan Divac – Faculty of technical sciences Čačak, University of Kragujevac, Svetog Save 65, 32000 Čačak, Serbia, (e-mail: srdjan.divac@ftn.kg.ac.rs).

Branko Koprivica – Faculty of technical sciences Čačak, University of Kragujevac, Svetog Save 65, 32000 Čačak, Serbia, (e-mail: branko.koprivica@ftn.kg.ac.rs).

 ISBN 978-86-7466-930-3

frequency of 1 Hz for controlled sinusoidal shape of $B(t)$ (voltage induced at the secondary winding). Measurements have been made for $B(t)$ amplitudes ranging from 0.2 T to 1.6 T with step of 0.2 T. The obtained hysteresis loops are presented in Fig. 1. Also, $H(t)$ and B(t) have been measured at 50 Hz and 1 T to obtain a dynamic hysteresis loop needed for calculation of phenomenological parameters of $H_{exc}(t)$. This hysteresis loop is shown in Fig. 1 as dashed line.

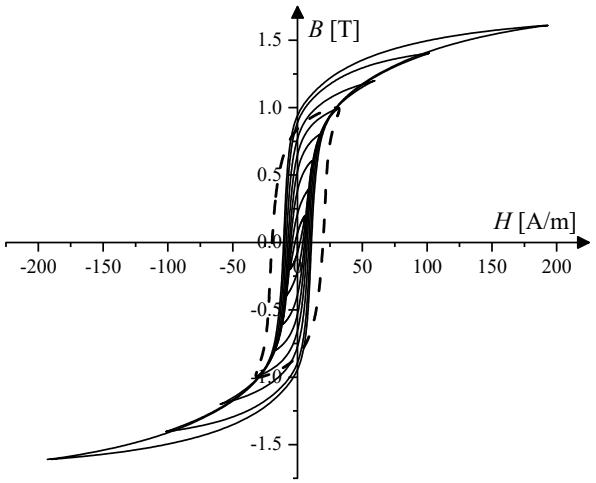

Fig. 1. Measured hysteresis loops for sinusoidal shape of $B(t)$.

III. Simulation Procedure

Considered electric circuit consisting of voltage source $u(t)$ in series with linear resistor R, linear inductor L and nonlinear inductive element exhibiting hysteretic properties L_h is presented in Fig. 2.

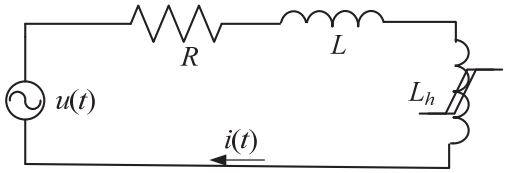

Fig. 2. Electric AC circuit with linear R and L elements and nonlinear L_h element with hysteresis.

Solving of this circuit means the calculation of its electric current $i(t)$, which depends on elements R, L and L_h and their characteristics. Obtaining dynamic solution is complicated due to the nonlinear and hysteretic characteristic of L_h. Its characteristic is usually represented with the dynamic hysteresis loops (the dynamic magnetic field $H_{dyn}(t)$ and magnetic flux density $B(t)$).

A. Calculation of dynamic magnetic field $H_{dyn}(t)$

Dynamic magnetic field $H_{dyn}(t)$ can be obtained by calculating its quasistatic $H_{qs}(t)$, eddy current $H_{eddy}(t)$ and excess $H_{exc}(t)$ components, and summing them up [10, 12]:

$$H_{dyn}(t) = H_{qs}(t) + H_{eddy}(t) + H_{exc}(t) \qquad (1)$$

Calculation of $H_{qs}(t)$ requires two steps. First, quasistatic field $H_{int}(t)$ needs to be calculated for sinusoidal $B(t)$, $B_{int}(t)$, with the amplitude $B_{\max}$ of interest. So, N harmonic components (amplitudes and phases) of measured quasistatic $H(t)$ need to be calculated at particular amplitudes of $B(t)$ for each measured quasistatic loop, Fig. 1. For new $B_{\max}$ of interest, N new harmonics of $H_{int}(t)$ can be calculated by linear or higher order polynomial interpolation of previously calculated harmonics [8]. Further, $H_{int}(t)$ and a new quasistatic hysteresis loop formed by $H_{int}(t)$ and sinusoidal $B_{int}(t)$ can be obtained. In the second step, a general solution for $H_{qs}(t)$ for non-sinusoidal $B(t)$, $B_{Lh}(t)$, with the amplitude of $B_{\max}$, can be obtained by using inverted hysteresis loop $H_{int}(B_{int})$, which can be considered as rate-independent (having fixed shape) at the frequency of 1 Hz. The shape of that hysteresis loop is only determined by the amplitudes of $H(t)$ and $B(t)$ and not by the shape of their waveforms [9]. Thus, $H_{qs}(t)$ can be obtained by reconstructing data points for $B_{Lh}(t)$ over data points for $H_{int}(B_{int})$ [13]. This procedure is illustrated in Fig. 3.

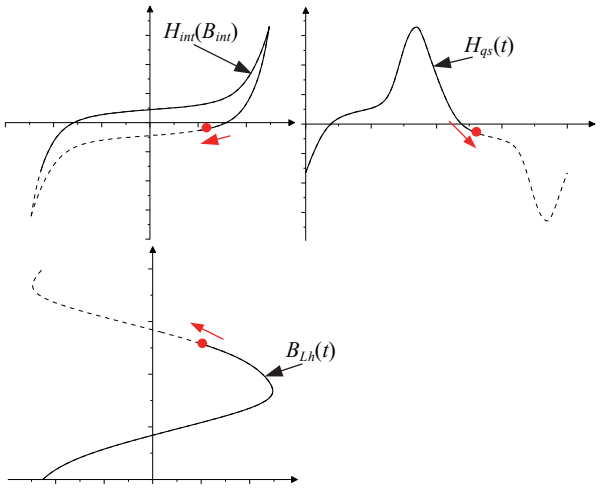

Fig. 3. Illustration of obtaining $H_{qs}(t)$ by reconstructing of non-sinusoidal $B_{Lh}(t)$ over the quasistatic hysteresis loop $H_{int}(B_{int})$.

Calculation errors may occur during this step due to the phase difference between $B_{Lh}(t)$ and B_{int}(t). This phase difference can be taken into account by delaying $B_{Lh}(t)$ for the period of Δt, $B_{Lh}(t+\Delta t)$, and proceed further with the calculations. Delaying period should be chosen so that the minimum and maximum values of $B_{Lh}(t+\Delta t)$ occur at the same time as for $B_{int}(t)$. Resulting $H_{qs}(t+\Delta t)$ should be delayed for the period of $-\Delta t$ to obtain $H_{qs}(t)$.

Waveform of $H_{eddy}(t)$ can be calculated from well-known analytical expression [10]:

$$H_{eddy}(t) = \frac{\sigma d^2}{12}\frac{\mathrm{d}B_{Lh}(t)}{\mathrm{d}t}, \qquad (2)$$

where σ is the conductivity of steel sheet and d is its thickness.

 ISBN 978-86-7466-930-3

Calculation of $H_{exc}(t)$ can be made using the following expression [10]:

$$H_{exc}(t)=\frac{n_0V_0}{2}\left(\sqrt{1+\frac{4\sigma GS}{{n_0}^2V_0}\frac{\mathrm{d}B_{Lh}(t)}{\mathrm{d}t}}-1\right), \quad (3)$$

where G is equal to 0.1356 and n_0 and V_0 are phenomenological parameters of material.

Consideration of hysteresis loop measured at 1 Hz as rate-independent is not completely correct (accurate), as there would always exist some difference between such loop and true static loop due to the existence of the dynamic components of the field ($H_{eddy}(t)$ and $H_{exc}(t)$). Dynamic components at 1 Hz participate with several percent in the quasi-static field and power loss under sinusoidal and non-sinusoidal conditions [14]. However, these components are much smaller at 1 Hz than at 50 Hz, considered in the simulations. Accordingly, the accuracy of the simulation would not be significantly affected with such consideration (approximation).

It should be noted that all quantities measured and calculated (magnetic field and flux density) are averaged for the considered mean magnetic path length and cross-section area of the toroidal sample. Actually, these quantities vary with the radial distance from the sample longitudinal axis (over the radius). However, the variations are not too high when the outer to inner radius ratio (r_2/ r_1) is low, as in the case of used sample (see Table I). The results of the simulation relate to the sample as a whole, as a part of the considered electric circuit, neglecting inhomogeneity of the magnetic field, which is acceptable in most of the practical applications. Accordingly, expressions (2) and (3) do not depend on the toroid dimensions (radiuses r_1 and r_2 and width w).

B. Iterative procedure

Proposed iterative algorithm for solving the circuit presented in Fig. 2 can be divided into the following steps:

1) calculating of the voltage at L_h for (i+1)-th iteration, $u_{Lh,i+1}(t)$, using II Kirchhoff's law [15]:

$$u_{Lh,i+1}(t)=u(t)-Ri_i(t)-L\frac{\mathrm{d}i_i(t)}{\mathrm{d}t}, \quad (4)$$

where $i_i(t)$ is the current derived from i-th iteration, t is the time, R and L are the resistance and inductance of the considered linear elements,

2) calculation of $B_{Lh,i+1}(t)$ from $u_{Lh,i+1}(t)$ using Faraday's law [15], as follows:

$$B_{Lh,i+1}(t)=\frac{1}{N_1S}\int_0^t u_{Lh,i+1}(t)\mathrm{d}t, \quad (5)$$

where N_1 is the number of turns in the magnetising coil and S is the cross-section area of magnetic core of L_h,

3) calculation of $H_{dyn,i+1}(t)$ for non-sinusoidal $B_{Lh,i+1}(t)$ using the procedure explained in subsection A,

4) calculation of $i_{i+1}(t)$ using Ampere's law [15]:

$$i_{i+1}(t)=\frac{H_{dyn,i+1}(t)}{N_1}l_c, \quad (6)$$

where l_c is the mean magnetising path length of L_h,

5) steps 1-4 should be repeated until condition (7) is met:

$$\frac{\max\{|i_i(t)|\}-\max\{|i_{i+1}(t)|\}}{\max\{|i_{i+1}(t)|\}}100\%<\varepsilon, \quad (7)$$

where ε is predetermined limit, which is not so rigorous.

Iterative procedure starts with $i_0(t)$=0 A for each time sample of t>0 and amplitude of $u(t)$ factorised by K>1 to minimise the oscilations and time shifts between iterations, such that:

$$U_{m,k}=\frac{U_m}{K}k, \quad (8)$$

where k=1, 2, 3,…, K. Solution of the k-th step is the new initial condition $i_k(t)$ for the (k+1)-th step. The value of K should be chosen high enough to allow for good convergence of the iterative procedure, but low enough to keep required computation time acceptable.

After finishing the iterative procedure, obtained waveforms of $H_{dyn}(t)$ and $B_{Lh}(t)$ can be used to plot dynamic hysteresis loop of L_h. Also, the specific power loss of L_h (corresponding to the area of the dynamic hysteresis loop), expressed in W/kg, can be calculated as:

$$P_s=\frac{1}{mT}\int_0^T u_{L_h}(t)i(t)\mathrm{d}t=\frac{Sl_c}{mT}\int_0^T\frac{\mathrm{d}B_{L_h}(t)}{\mathrm{d}t}H_{dyn}(t)\mathrm{d}t, \quad (9)$$

where T=1/f is the period and m is the mass.

IV. Simulation Results

Four cases of the electric circuit presented in Fig. 2 have been considered:

I. with R=0 Ω and L=0 H;
II. with R=48 Ω and L=0 H;
III. with R=0 Ω and L=20 mH and
IV. with R=48 Ω and L=20 mH.

A sinusoidal voltage source with U_m from 2 V to 10 V with the step of 2 V and frequency of 50 Hz has been used for all performed simulations. All simulations have been made using 1000 data points.

Other, lower or higher frequencies can also be used in simulations. However, the frequency of 50 Hz is of particular importance, as it is used as the working frequency in most of the basic electric circuits, as considered one. Consideration of higher frequencies would also be interesting for some advanced applications of electric machines and drives, power

 ISBN 978-86-7466-930-3

electronics and other. However, that is beyond of the scope of this paper.

Total of N=35 harmonics of measured quasistatic $H(t)$ have been used during the 4th step of the simulation process. This number of harmonics has been found to be optimal in case of U_m=10 V, therefore, less harmonics could be used for lower U_m.

Parameters of the electrical steel σ and d, used to calculate the magnetic field of eddy currents in (2), have been provided by the manufacturer and amount 2083 kS/m and 0.27 mm, respectively. Other parameters of the material given by the producer are: density ρ=7650 kg/m^3, B_{max}=1.90 T for H_{max}=800 A/m, specific power loss at 50 Hz is 0.72 W/kg for 1.5 T and 0.95 for 1.7 T, maximum of the relative permeability is around 70000 for static fields, coercive field goes up to 10 A/m for static field and up to 25 A/m for field at 50 Hz under sinusoidal $B(t)$.

Parameters n_0=908 and V_0=0.08 A/m in (3) have been obtained by fitting the excess power loss caused by $H_{exc}(t)$ for sinusoidal shape of $B(t)$ at 1 T to the excess power loss calculated from measurements for the same $B(t)$ [12], taking into account both hysteresis and dynamic loss (given by the hysteresis loops measured at 1 Hz and 50 Hz) and eddy current loss calculated using $H_{eddy}(t)$ given by (2) at 50 Hz. Fitting has been performed using the criteria of RMSD between excess power loss produced by fitted and calculated excess magnetic field. Both parameters have been kept constant in all performed simulations.

Predetermined limit ε has been set to 0.5%. This value has been chosen in order to obtain best convergence of the simulation procedure. Parameter K has been set to 30 to obtain best solutions in case III for U_m=10 V and has been kept at this value for all simulations. It has been found that total number of iterations for K steps is 36, 30, 31 and 30, for each of the considered cases at U_m=10 V, respectively.

Results for $i(t)$ for case IV of electric circuit for all considered values of U_m are presented in Fig. 4.

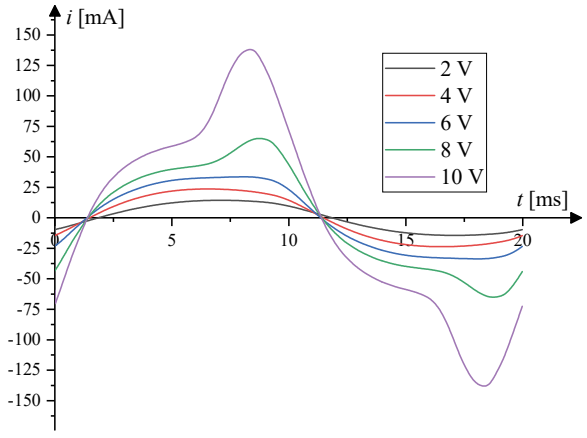

Fig. 4. Simulated $i(t)$ waveforms for the case of R=48 Ω and L=20 mH, for all considered values of U_m.

Influence of linear circuit elements R and L to the solution of the circuit for considered cases I-IV is better seen in observing the hysteresis loops of L_h than in observing $i(t)$. Therefore, a number of simulated hysteresis loops has been constructed and the loops have been compared to observe such influence.

Simulated hysteresis loops for each of the considered cases of circuit and all values of U_m are presented in Fig. 5-8, respectively. Scales are the same in all these figures for better illustration of R and L influence.

It can be seen that in all of the presented cases simulated hysteresis loops for lower U_m are fully encompassed by the hysteresis loops of higher U_m. This is in accordance with the hysteresis theory which states that hysteresis loops obtained for higher voltages, under same conditions, should encompass the ones at lower voltages [10].

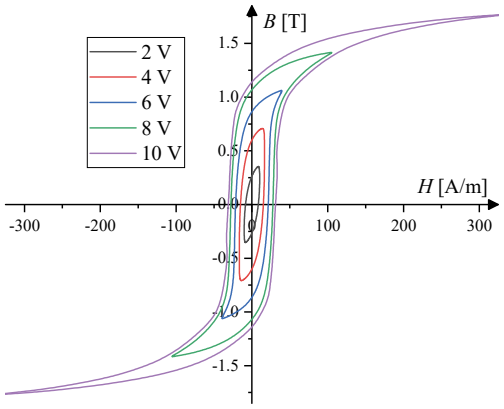

Fig. 5. Simulated hysteresis loops for the case of R=0 Ω and L=0 mH, for all considered values of U_m.

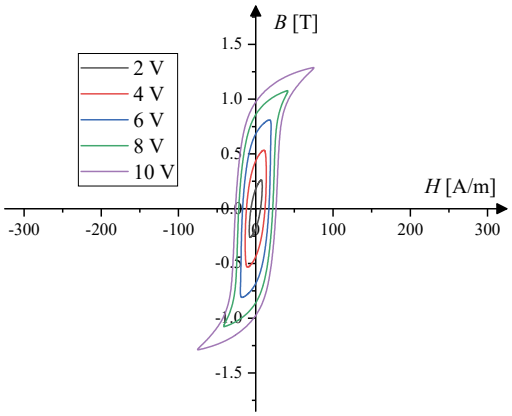

Fig. 6. Simulated hysteresis loops for the case of R=48 Ω and L=0 mH, for all considered values of U_m.

Hysteresis loops for all considered cases of electric circuit at particular values of U_m are presented in Fig. 9-13, respectively.

At lower voltages, Figs. 9 and 10, the used electrical steel exhibits almost linear behaviour, therefore resulting in almost elliptical loops and sinusoidal $i(t)$. This limits the influence of L in (4) since its voltage is proportion to the rate of change of $i(t)$. Also, adding R in the electric circuit results in lover voltage levels at L_h. Its influence is more noticeable than the L's, since the voltage over the resistor is proportional to the $i(t)$.

 ISBN 978-86-7466-930-3

Simulations at higher voltages, Figs. 11-13, show greater influence of nonlinearity of the material, causing the significant peaks in the $i(t)$. Influence of L is more prominent under these conditions, resulting in smoother $i(t)$ in case III than in case I by effectively lowering its peaks. Choking of the current [15] is less prominent in case IV since in this case linear R causes lower voltage levels at L_h-lesser influence of nonlinearity on the shape of $i(t)$, making it smoother.

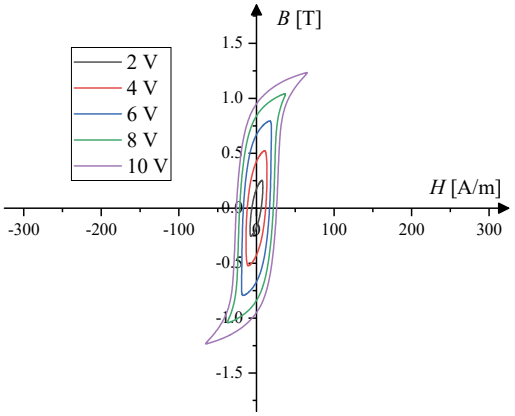

Fig. 7. Simulated hysteresis loops for the case of R=0 Ω and L=20 mH, for all considered values of U_m.

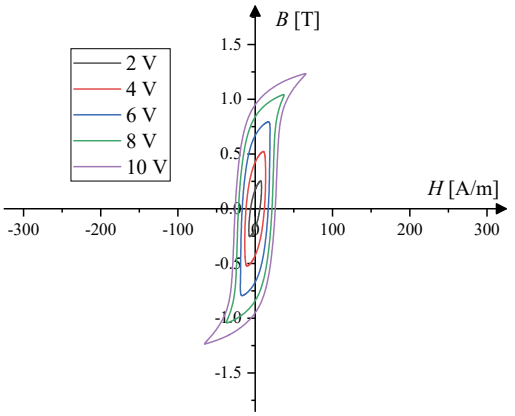

Fig. 8. Simulated hysteresis loops for the case of R=48 Ω and L=20 mH, for all considered values of U_m.

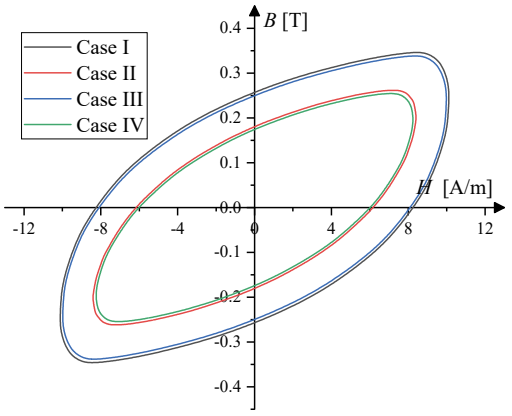

Fig. 9. Simulated hysteresis loops for U_m=2 V for all considered cases of electric circuit.

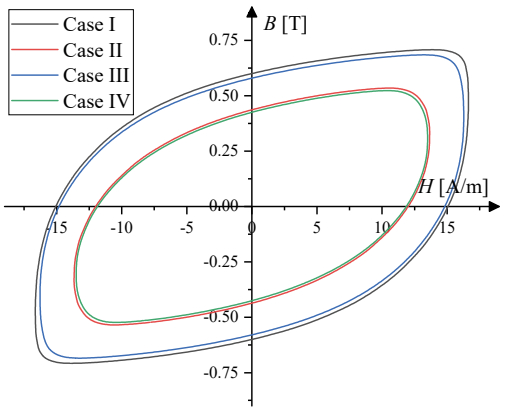

Fig. 10. Simulated hysteresis loops for U_m=4 V for all considered cases of electric circuit.

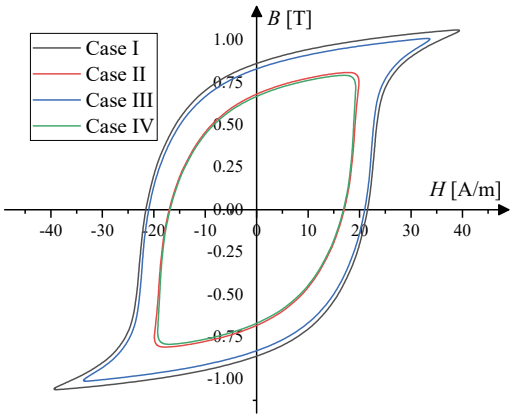

Fig. 11. Simulated hysteresis loops for U_m=6 V for all considered cases of electric circuit.

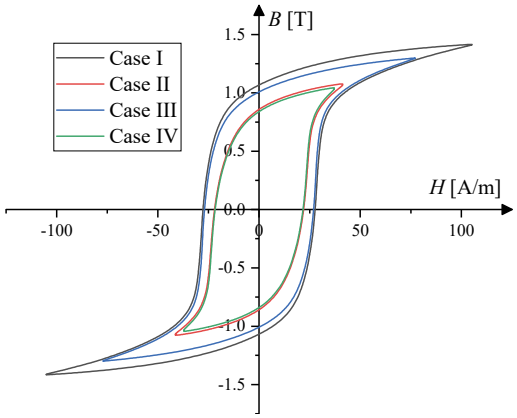

Fig. 12. Simulated hysteresis loops for U_m=8 V for all considered cases of electric circuit.

According to the results presented, simulation method presented could be suitable for solving electric circuits with L_h for sinusoidal $u(t)$ in the steady state time domain. The simulation method presented has not been tested in simulation of transient processes.

 ISBN 978-86-7466-930-3

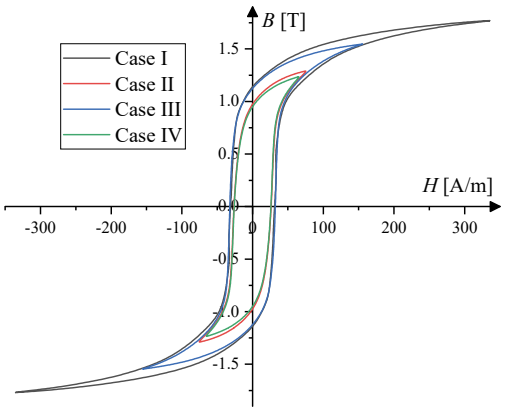

Fig. 13. Simulated hysteresis loops for U_m=10 V for all considered cases of electric circuit.

V. Conclusion

A simulation method for solving electric circuits with nonlinear inductor with hysteresis in time domain has been resented in this paper. The considered electric circuit consisted of AC voltage source connected in series with linear resistor, linear inductor and nonlinear inductor with hysteresis. Proposed calculation procedure has been based on solving an equation derived from Kirchhoff's law through series of successive iterations. Influence of the inductor with hysteresis has been accounted for by calculating current in the electric circuit from its $H_{dyn}(t)$ corresponding to the $B_{Lh}(t)$ from iteration. Waveform of $H_{dyn}(t)$ has been calculated as the sum of its quasistatic, eddy current and excess magnetic field components. Each component has been calculated separately for the considered $B_{Lh}(t)$.

Measurements have been made for $H(t)$ at low frequency of 1 Hz for sinusoidal shape of $B(t)$ for amplitude from 0.2 T to 1.6 T with the measurement step of 0.2 T. Also, measurements have been made at 50 Hz for the sinusoidal $B(t)$ of 1 T.

Simulations have been performed for sinusoidal voltage source with the amplitudes from 2 V to 10 V with the step of 2 V. Also, four cases of the electric circuit have been considered for each of the voltages-without, with one and with both linear elements. Based on the simulation result and their discussion, it can be concluded that the presented simulation method could be suitable for solving electric circuits with nonlinear inductors with hysteresis in steady state time domain.

Acknowledgment

This study was supported by the Ministry of Education, Science and Technological Development of the Republic of Serbia, and these results are parts of the Grant No. 451-03-68/2022-14/200132 with University of Kragujevac - Faculty of Technical Sciences Čačak.

References

[1] B. Koprivica, A. Milovanović, M. Đekić, "Effects of Wound Toroidal Core Dimensional and Geometrical Parameters on Measured Magnetic Properties of Electrical Steel", Serbian Journal of Electrical Engineering, vol. 10, no. 3, pp. 459-471, Oct. 2013.

[2] A. Rezaei-Zare, R. Iravani, "On the Transformer Core Dynamic Behavior During Electromagnetic Transients", *IEEE Transactions on Power Delivery*, vol. *25*, no. *3*, pp. *1606-1619*, July 2010.

[3] F. G. Montoya, F. De Leon, F. Arrabal-Campos, A. Alcayde, "Determination of Instantaneous Powers from a Novel Time-Domain Parameter Identification Method of Non-Linear Single-Phase Circuits", *IEEE Transactions on Power Delivery* (Early Access), Dec. 2021.

[4] J. H. B. Deane, "Modelling the Dynamics of Nonlinear Inductor Circuits", *IEEE Transactions on Magnetics*, vol. *30*, n0. *5*, pp. *2795 – 2801*, Sept. 1994.

[5] I. D. Mayergoyz, "*Mathematical Models of Hysteresis and Their Applications*", Elsevier Science, New York, USA, 2003.

[6] A. R. P. J. Vijn, O.Baas, E. Leepelaars, "Parameter Estimation for the Jiles–Atherton Model in Weak Fields", *IEEE Transactions on Magnetics*, vol. *56*, no. *4*, April 2020.

[7] A. S. Q. Antonio, F. R. Fulginer, A. Laudani, A. Faba, E. Cardelli, "An Effective Neural Network Approach to Reproduce Magnetic Hysteresis in Electrical Steel Under Arbitrary Excitation Waveforms", *Journal of Magnetism and Magnetic Materials,* vol. *528*, June 2021.

[8] S. Divac, B. Koprivica, "Simulation of Dynamic Hysteresis Loops for Toroidal Sample for Sinusoidal Shape of Magnetic Flux Density", 21st International Symposium INFOTEH-JAHORINA, 16-18. March 2022.

[9] D. Makaveev, L. Dupre, M. De Wulf, J. Melkebeek, "Modelling of Rate-Independent Hysteresis with Feed-Forward Neural Networks", Conf. Proc. Neural Networks and Appl., Interlaken, Switzerland, pp. 3451-3456, Feb. 2002.

[10] G. Bertotti, "*Hysteresis in Magnetism for Physicists, Material Scientists and Engineers*", Academic Press, New York, USA, 1998.

[11] C. D. Schunn, D. Wallach, "Evaluating Goodness-of-Fit in Comparison of Models to Data", pp. *115-135*, 2005. In W. Tack (Ed.), Psychologie der Kognition: Reden and Vorträge anlässlich der Emeritierung von Werner Tack, Saarbrueken, Germany, University of Saarland Press.

[12] B. Koprivica, S. Divac, "Analysis and Modeling of Instantaneous Magnetizing Power of Ferromagnetic Core in Time Domain", *IEEE Magnetic Letters*, vol. *12*, p. *2103505*, Sept. 2021.

[13] J. Takacs, "Hysteresis Loop Reversing by Applying Langevin Approximation", *The International Journal for Computation and Mathematics in Electrical and Electronic Engineering*, vol. *36*, no. *4*, July 2017.

[14] M. De Wulf, L. Dupre, J. Melkebeek, "Quasistatic Measurements for Hysteresis Modeling", Journal of Applied Physics, vol. 87, no. 9, pp. 5239-5241, May 2000.

[15] K. L. Kaiser, "*Electromagnetic Compatibility Handbook*", CRC Press, New York, USA, 2004.

 ISBN 978-86-7466-930-3